CONNECTIVITY OF FRACTURE NETWORKS: THE EFFECTS OF ANISOTROPY AND SPATIAL CORRELATION

MOHSEN MASIHI[1], P. R. KING[1], P. R. NURAFZA[1]
[1]Department of Earth Science & Engineering, Imperial College, Exhibition Road, London, SW7 2AZ, UK, Email: mohsen.masihi@imperial.ac.uk

ABSTRACT

In fractured formations of very low matrix permeability, connectivity of fractures is a crucial parameter which may affect the overall flow significantly. Percolation theory introduces a quantitative scaling approach from which the connectivity and its associated uncertainty can be estimated very rapidly. However, the usual scaling laws do not consider anisotropies or spatial correlations which in turn are the characters of natural fractures. The main contribution of this work is first to derive and verify numerically the scaling including the effects of anisotropy for a simple fracture model with a bi-modal orientation distribution. Secondly, we use a correlated fracture model based on the idea that the elastic free energy due to the fracture density follows a Boltzmann distribution to address the effects of fracture spatial correlation on the connectivity of the system. As a result this extends the applicability of the percolation approach to anisotropic as well as correlated fracture systems which may improve our predictive capability relating to the flow behaviour for real field problems.

1. INTRODUCTION

Fractures, by which we mean any discontinuity within a rock mass that develop as a response to stress, are important for flow movement in hydrocarbon reservoirs or aquifers. As the available data related to the fracture geometries are so limited, there will be a great deal of uncertainty in the spatial distribution of fractures which affect their connectivity and so field performance. The conventional approach to quantify these effects is to build a number of possible detailed reservoir models using available data, upscale them and perform flow simulations. This is clearly computationally very expensive. Therefore, there is a need for much simpler models, especially for engineering purposes.

Alternatively, a "*percolation approach*" can be used when a strong permeability contrast exists in the system. Imagine a reservoir model constructed with an object based technique, where geometrical objects are placed randomly in space. Then the connectivity can be estimated directly by percolation theory extremely rapidly. In particular the percolation approach is able to estimate the uncertainty which is not possible with a single realization reservoir model. This approach has been applied to non fractured oil reservoirs to estimate reservoir performance [King, 1990; King et al. 2001]. However, the extension of this approach to fractured rocks is not straightforward due to the complexity of fractures. In nature, fractures appear on various scales and interact mechanically which results in certain correlations in their geometrical properties (e.g. fracture sets due to tectonic events). This work aims to extend the applicability of the percolation approach to anisotropic as well as correlated fracture systems. This paper is organized as follows: A review of the basics of the percolation approach is presented. We describe how to account for the anisotropy in fracture

orientation in a simple fracture model with bi-modal orientation distribution. We then describe a correlated fracture model which uses the resulting expression for the spatial correlation in the elastic displacement of fractures as an energy term inside the simulated annealing algorithm to generate realizations of fractures. The connectivity of this model will then be compared with the connectivity results from the uncorrelated fractures. This is followed by conclusions.

2. THE PERCOLATION APPROACH

Percolation theory is a mathematical model which relates the global connectivity to the number density of objects randomly distributed in the region. Consider an infinite lattice of sites occupied with a probability p where neighbouring occupied sites form clusters. There is a unique occupancy (percolation threshold, p_c^∞) below which a system is not connected while above p_c^∞ there is a percolating cluster which spans the whole system. Around p_c^∞ the probability that a site belongs to the spanning cluster $P(p)$ and the correlation length $\xi(p)$ have respectively the scaling $P(p) \propto (p - p_c^\infty)^\beta$ and $\xi(p) \propto | p - p_c^\infty |^{-\nu}$. The exponents β and ν are universal and have the value 5/36 and 4/3 respectively in 2D [Stauffer and Aharony, 1992]. However the percolation threshold does depend on the detail of the system.

In a finite system (i.e. a lattice of size $L \times L$) due to a sample size uncertainty there may be one or more clusters that span the system appearing at different values of p. This leads to the concept of an apparent threshold $\tilde{p}_c$ which depends on the system size L. We define connectivity $P(p,L)$ as the fraction of occupied sites belonging to the spanning clusters. From results of $P(p,L)$ at a particular p and system size obtained over a large number of realizations it is easy to determine the mean value $P(p,L)$ (the same notation as before) and the fluctuations about the mean $\Delta(p,L)$ (standard deviation). Different results can then be related to each other through the finite size scaling laws [Stauffer and Aharony, 1992],

$$P(p,L) = L^{-\beta/\nu} \Im[(p - p_c^\infty) L^{1/\nu}] \quad (1)$$

$$\Delta(p,L) = L^{-\beta/\nu} \Re[(p - p_c^\infty) L^{1/\nu}] \quad (2)$$

These scaling transformations provide two universal curves $\Im$ and $\Re$ from which one can easily predict the mean connectivity and its associated uncertainty without performing any explicit realizations. Extensive studies have shown the applicability of percolation theory to fracture systems [e.g. Berkowitz, 1995; Adler and Thovert, 1999]. In particular, the effects of fracture length [e.g. Charlaix et al. 1984; Bour and Davy 1997; Mourzenko et al. 2005] and orientation distribution [e.g. Robinson 1984; Balberg et al. 1984; Masihi et al. 2005] on the scaling laws of connectivity have been investigated. However, there has been little investigation on the spatial correlation of fractures which mainly concentrated on the long range fracture density correlations modelled by fractal geometry [e.g. Darcel et al. 2003].

3. A SIMPLE FRACTURE MODEL

Consider a square of size $L \times L$ in which line segments representing fractures are placed following Poisson statistics. All fractures have the same length l but their orientations are

distributed in two families (sets) of parallel fractures. The isotropy of this system is achieved by implanting randomly one horizontal fracture for every vertical fracture. The percolation parameter (the term equivalent to the occupancy probability) is $p = 1 - \exp\left(-N\langle a_{ex}\rangle / 4L^2\right)$ as used by Masihi et al. [2005]. The average excluded area is $\langle a_{ex}\rangle = l^2/2$ and the average projected length of fractures in the x direction is $\langle l_x\rangle = l/2$. Therefore the effective length scale, defined as $L/\langle l_x\rangle$, is $L_x = 2L/l$. The percolation probability, defined as the likelihood of a fracture being connected to the spanning clusters is, $P(p,L) = n_s / n_w$ where n_s and n_w are respectively the number of fractures in the spanning cluster and in the whole network.

We use the standard labelling algorithm to recognize clusters and update their statistics as the simulation progresses. A plot of the mean connectivity $P(p,L)$ obtained from different system sizes as a function of p which gives different curves is shown in Figure 1a. From the finite size dependency of apparent threshold $\tilde{p}_c$, defined as a point when 50% of realisations percolate, we found $p_c^{\infty} \approx 0.538$. Using the standard values for the critical exponents, we can use the scaling (1) to relate all the mean connectivity curves to a single curve called universal mean connectivity curve $\Im$ (Figure 1b). Similarly the numerical results and the scaling (2) can be used to get the universal standard deviation of connectivity curve $\Re$.

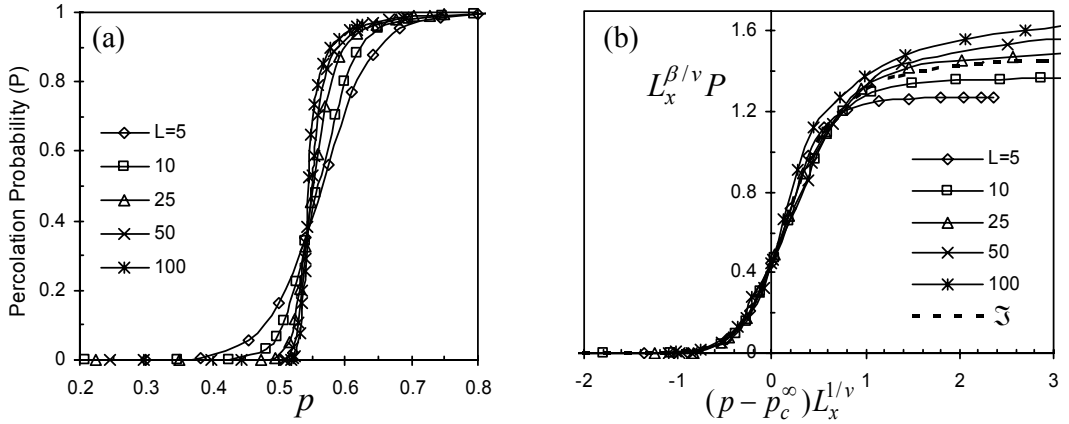

FIGURE 1. Mean connectivity curves for the horizontal-vertical fracture model ($l = 1$) for five different system sizes: (a) unscaled results and (b) rescaled results using the scaling transformations (1) from which the universal mean connectivity $\Im$ can be determined.

4. ANISOTROPY

We introduce anisotropy in the above model by implanting one fracture with angle θ_o from the horizontal for every horizontal fracture. The average excluded area is $l^2 \sin\theta_o / 2$. The average projected length of fractures in the x and the y directions are $\langle l_x\rangle = (l + l\cos\theta_o)/2$ and $\langle l_y\rangle = (l\sin\theta_o)/2$ respectively. We define the aspect ratio representing anisotropy of the system as $\omega = L_x / L_y = \sin\theta_o / (1 + \cos\theta_o)$. The rest of the model is identical to the isotropic horizontal-vertical fracture model. Now we look at the finite size scaling. If we rescale the

horizontal and vertical average connected fraction with L_x using scaling (1) for a fixed aspect ratio similar to the work by Masihi et al. [2005], we find that again there is a data collapse but in two sets of results. The horizontal and vertical mean connectivity curves are displaced in two opposite directions from the isotropic curve. To bring back the horizontal and vertical connectivity curves to the isotropic curve, we then use the apparent threshold $\tilde{p}_c$, which scales as $\tilde{p}_{ci}(\omega, L) = p_c^{\infty} + \Lambda_i(\omega) L_x^{-1/\nu}$, instead of the infinite threshold in equation (1). There is a symmetry relation between connectivity in the *x* direction for aspect ratio ω and that in the *y* direction for aspect ratio 1/ ω. The results shown in Figure 3a also show another symmetry for the shift in the apparent threshold about the isotropic case, $\Lambda_x(\omega) = -\Lambda_y(\omega)$. These lead to the functional form $\Lambda(\omega) = c(\omega^{1/\nu} - 1)$ for the shift in the apparent threshold which is verified numerically (Figure 2b). This enables us to use the previously determined universal connectivity curve for this anisotropic fracture system. Similarly the scaling for $\Delta(p, L)$ uses the same apparent threshold as well as a change in magnitude which can be accounted for by rescaling with the geometric mean length, $\Delta(p, L) = \omega^{1/2} L_x^{-\beta/\nu} \Re[(p - \tilde{p}_c) L_x^{1/\nu}]$.

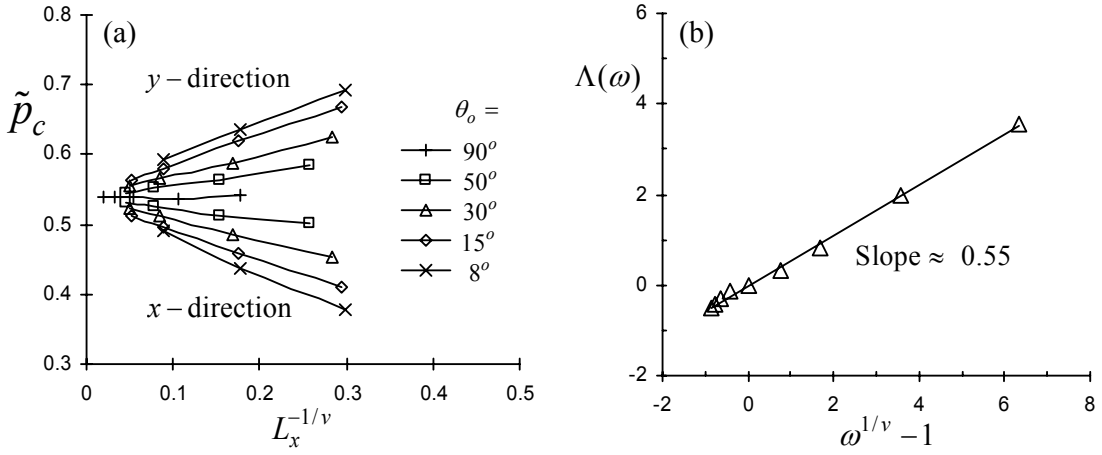

FIGURE 2. Determination of the shift in the apparent threshold Λ: (a) The slope for θ_o = 90°, 50°, 30°, 15° and 8° provides $\Lambda \approx 0.005$, 0.14, 0.3, 0.43 and 0.53 respectively and (b) Variation of Λ against $\omega^{1/\nu} - 1$ which satisfied the scaling $\Lambda = c(\omega^{1/\nu} - 1)$ with $c \approx 0.55$.

5. SPATIAL CORRELATION

A correlated fracture network is made by using the resulting expression for the spatial correlation in the elastic displacement of fractures as an objective function inside a simulation annealing algorithm. The same basic methodology of the percolation approach is then applied to analyse the connectivity of the presented correlated fracture model.

5.1 Correlation in elastic displacement of fractures.

We shall assume that everywhere the displacement vector u has a continuous (or elastic u^e) part and a discontinuous (or inelastic u^i) part which acts as a source of inelastic strain. Similarly the strain and stress can be decomposed into their elastic and inelastic parts,

$e_{ij} = e^e_{ij} + E_{ij}$ and $\sigma_{ij} = \sigma^e_{ij} + S_{ij}$ respectively. The stress/strain relation from Hook's law is $\sigma^e_{ij} = \lambda e^e_{ii}\delta_{ij} + 2\mu e^e_{ij}$ where the strain for small deformation is $e^e_{ij} = (\partial_j u^e_i + \partial_i u^e_j)/2$ [Landau and Lifshitz, 1959]. In the absence of body forces, the equation of continuity for isotropic body is,

$$\partial_j \sigma_{ij} = \partial_j \sigma^e_{ij} + \partial_j S_{ij} = 0 \qquad \text{or} \qquad \partial_j \sigma^e_{ij} = -\partial_j S_{ij} \tag{3}$$

where the term $-\partial_j S_{ij}$ can be interpreted as a *"fictitious"* body force that keeps the fracture open. This term can thus be viewed as a random input driving force-giving rise to fracturing. Now we look at the stochastic solution to equation (3) which determines σ^e_{ij} and e^e_{ij}.

Elastic energy, the work done by the elastic forces on the total strain, is $E = \sigma^e_{ij} e^e_{ji}/2$. We hypothesise that the frequency probability of the strain energy due to the dislocation density follows a Boltzmann distribution $P(E) \propto \exp(-E/kT)$ assuming that the dislocations adopt a configuration that maximises the entropy of the system subject to the mean energy being fixed. This leads to the expression for the spatial correlation in the elastic displacement [see Heffer and King, 2005], $\left\langle u^e_i(r) u^e_j(-r) \right\rangle = A.[\eta.\delta_{ij} + r_i.r_j/r^2]/r$ where $A = \langle E \rangle / 16\pi\mu(1-\upsilon)$, $\eta = 3 - 4\upsilon$ and δ_{ij} is the Kroneker delta. The terms $\langle E \rangle$, μ, υ are respectively the average strain energy, the shear modulus and the Poisson ratio of the rock. This covariance function can be written in vector forms as $\left\langle u^e_i(r) u^e_j(-r) \right\rangle = A.[\eta.(u_i,u_j)/r + (r,u_i).(r,u_j)/r^3]$ where (u_i,u_j) indicates the scalar product of two vectors u_i and u_j representing two fractures at points i and j with a distance vector r. If we represent fractures with line segments in 2D instead of vectors we end with,

$$\left\langle u^e_i(\boldsymbol{r}) u^e_j(-\boldsymbol{r}) \right\rangle = A.u_i.u_j.[\eta.|\cos(\theta_j - \theta_i)| + |\cos(\alpha - \theta_i)\cos(\alpha - \theta_j)|]/r_{ij} \tag{4}$$

where α, θ_i and θ_j are respectively the orientation of distance vector r and fractures u_i and u_j with respect to the horizontal. Finally, random functions simulated with this covariance will satisfy the equation of continuity (3).

5.2 Simulation annealing.

We use simulated annealing to find an appropriate pattern of fractures that honours their correlation given by equation (4). This optimization technique uses the Boltzmann probability distribution, $P(E) \propto \exp(-E/kT)$ to get out of a local minimum in favour of finding a more global one [Aarts and Korst, 1989]. To apply simulated annealing to a given problem, one must define the following terms: (i) a set of possible configurations of the system (ii) a method for a small random change to the configuration (iii) an energy (or objective) function to be minimized and (iv) an annealing schedule of changing a temperature-like parameter "T".

This process starts with an initial configuration at the initial temperature T_i (the same unit as the *"energy"*). The transition probability from the current state i with energy E_i to the new state j with energy E_j at a given temperature T is then assigned as follows. If $E_j - E_i \le 0$ state j is accepted as the current state unconditionally. Otherwise, state j will be accepted if $\exp[-(E_j - E_i)/T] > y$ where y is a uniform random number in the range $[0,1]$.

The system is optimized at each temperature by applying a series of accepted small random changes to the system. Finally the temperature will be lowered slowly using a geometric series $T_{k+1} = T_k R_k^k$ (e.g. $R = 0.97$) until no further changes occur while at each temperature stage the simulation should proceed long enough for the system to reach a steady state.

5.2.1 Simulation conditions.

The initial configuration of fractures is defined by distributing 1000 randomly oriented fractures in a square of size 100 following a Poisson distribution. We arbitrarily choose a Gaussian distribution for the fracture length (with mean and standard deviation equal to 33.3 and 10 respectively). To change a given fracture pattern, we randomly choose a fracture and change its orientation (a random number between -1 and 1 multiplied by $0.05 \times \pi$) and its position and length (a random number between -0.5 and 0.5). We define *"energy"* E to be the sum of the correlation function (4) among all pairs of fractures in the system. We use periodic boundary conditions with two similar cells in each direction and set $\eta = 2$ correspond to a typical value for the Poisson ratio of subsurface rocks $(\upsilon = 0.25)$. The initial temperature T_i is 500000 and the temperature decrement in each step is 4%. As the simulation progresses the average length of fractures in the system decreases from 33.3 at the initial state towards zero at the end of the simulation. Figure 4 shows a realization of fractures at the 160th temperature step, where the temperature and average length are about 759 and 3 respectively.

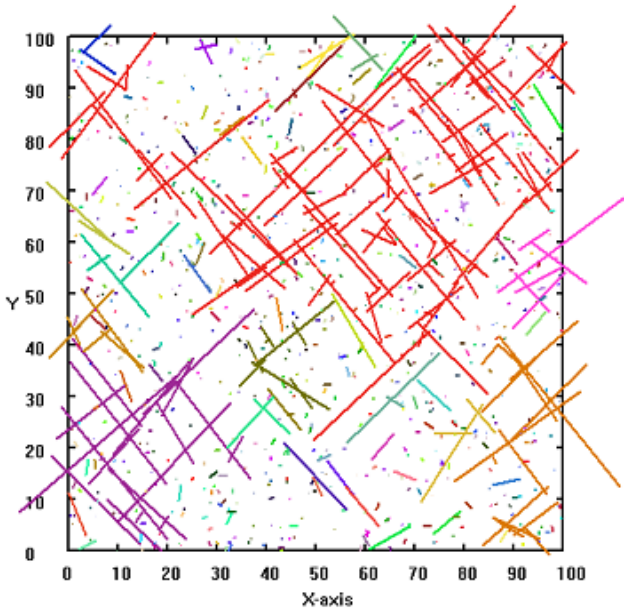

FIGURE 3. A realization of correlated fracture network picked at the 160th temperature step where the temperature and the average length of fractures are about 759 and 3 respectively.

Let us now exploit the statistics of this correlated fracture network. We classified the fractures into two groups: fractures with length larger and smaller than the average length of fractures. We found that small fractures are nearly randomly oriented whereas the larger fractures tend to be placed in the two perpendicular sets. This is because the energy change

due to the small fractures may be smaller than the energy penalty considered in the annealing algorithm. Moreover, the length distribution for fractures in this network was found to be matched with either a power-law or a negative exponential.

5.3 Connectivity of the correlated fracture network.

We repeat the above simulation many times with the same condition but using different random seeds to get reliable statistics of this correlated fracture model. For all realisations, we extract the fracture network at the temperature steps corresponding to the average fracture length 4, 3.5 and 3. The length distribution of fractures at these temperature steps is found to be nearly a power-law. Monte Carlo simulation results and the theoretical discussions in the literature [*e.g.* Balberg *et al.*, 1984; Berkowitz, 1995; Adler and Thovert, 1999; Masihi et al. 2006] show that the connectivity of a system with a length distribution can be controlled by an effective length defined as the square root of the second moment of length distribution. Therefore, the effective length for the fracture networks with the average fracture length 4, 3.5 and 3 is respectively 8.65, 7.88 and 7.14. We then calculate the horizontal and vertical connectivity (percolation probability) of each extracted network using the method described earlier. These enable us to determine the mean and standard deviation of connectivity at the average fracture length 4, 3.5 and 3 which was respectively 0.75±0.27, 0.41±0.32 and 0.21±0.30. We now rescale the connectivity results and compare with the uncorrelated results of the randomly oriented fracture model described by Masihi et al. 2005 (Figure 4a). There is an obvious difference between the connectivity results of correlated and uncorrelated fractures. We have already shown that the scaling exponents for a system with a very broad length distribution such as power law are dependent on the exponent of the power law [see Masihi et al. 2006, Figure 11]. From the statistics of the fracture length distribution in this correlated model, we estimate the critical exponents as $1/\nu = 0.4$ and $\beta/\nu = 0.09$. Using these new values of the critical exponents, the connectivity results for the correlated networks are now consistent with the prediction from uncorrelated fractures (Figure 4b). This allows us to use the previously determined universal connectivity curves of uncorrelated fractures [Masihi et al. 2005, Figure 7] for the correlated fracture models.

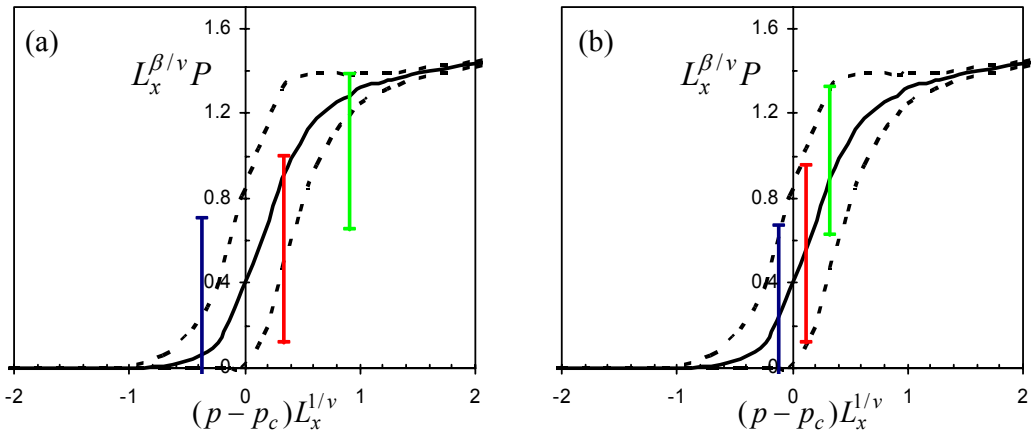

FIGURE 4. Comparison of connectivity of the correlated model with the average fracture length 4(green), 3.5(red) and 3(blue) with the uncorrelated universal P and $P \pm \Delta$ curves using: (a) standard values for the critical exponent and (b) $1/\nu = 0.4$ and $\beta/\nu = 0.09$.

6. CONCLUSION

We extended the applicability of the percolation approach to anisotropic as well as correlated fracture networks. We showed that the anisotropy in orientation of fractures does not alter the scaling exponents and so classic percolation applies. However, a previously determined "*apparent threshold*" must be used in the usual finite size scaling law of connectivity to account for the effects of the anisotropy. Moreover, we used the resulting expression for the spatial correlation in the elastic displacement of fractures as an objective function inside a simulated annealing algorithm to generate realizations of correlated fracture networks. The scaling exponents of connectivity of this correlated model were found to be different from the conventional, uncorrelated values.

Acknowledgments. The first author thanks the Iranian Ministry of Science, Research and Technology for sponsoring this research work as a part of his PhD studies at Imperial College.

REFERENCES

- Aarts, E., J. Korst (1989), *Simulated annealing and Boltzmann machines, a stochastic approach to combinational optimization and neural computing*, John Wiley & Sons, New York.
- Adler, P. M. and J. F. Thovert (1999), *Fractures and fracture networks*, Kluwer Academic Publishers, London.
- Balberg, I., C. H. Anderson, S. Alexander and N. Wagner (1984), Excluded volume and its relation to the onset of percolation, *Phys. Rev. B*, *30*(7), 3933-3943.
- Berkowitz, B. (1995), Analysis of fracture network connectivity using percolation theory, *Math. Geol.*, *27*(4), 467-483.
- Bour, O., and P. Davy (1997), Connectivity of random fault networks following a power law fault length distribution, *Water Resour. Res.*, *33*(7), 1567-1583.
- Charlaix, E., E. Guyon and N. Rivier (1984), A criterion for percolation threshold in a random array of plates, *Solid State Commun.*, *50*(11), 999-1002.
- Darcel, C., O. Bour, P. Davy and J. R. de Dreuzy (2003), Connectivity properties of two dimensional fracture networks with stochastic fractal correlation, *Water Resour. Res.*, *39*(10), 1272, doi: 10.1029/2002WR001628.
- Heffer, K. J., and P. R. King (2005), Spatial scaling of effective modulus and correlation of deformation near the critical point of fracturing, submitted to *Pure Appl. Geophys*.
- King P. R. (1990), The Connectivity and Conductivity of Overlapping Sandbodies, *North Sea Oil and Gas Reservoirs-II,* 353-361.
- King P. R., S. V. Buldyrev, N. V. Dokholyan, S. Havlin, Y. Lee, G. Paul, (2001), Predicting Oil Recovery Using Percolation Theory, *Pet. Geosci.*, *7*, 105.
- Landau, L. D., and E. M. Lifshitz (1959), *Theory of Elasticity*, pp. 134, Pergamon Press., London.
- Masihi, M., P. R. King and P. Nurafza (2005), Fast estimation of performance in fractured reservoirs using percolation theory, paper SPE 94186 presented at the 14th Biennial Conference, Madrid, Spain, June 13-16.
- Masihi, M., P. R. King and P. Nurafza (2006), Connectivity prediction in fractured reservoirs with variable fracture size: analysis and validation, paper SPE 100229 presented at the 15th Biennial Conference, Vienna, Austria, June 12-15.
- Mourzenko, V. V., J. F. Thovert and P. M. Adler (2005), Percolation of three dimensional fracture networks with power law size distribution, *Phys. Rev. E*, *72*, 036103.1-036103.14.
- Robinson, P. C. (1984), Numerical calculations of critical densities for lines and planes, *J. Phys. A: Math. Gen.*, *17*(14), 2823-2830.
- Stauffer, D., and A. Aharony (1992), *Introduction to percolation theory*, 181 pp, Taylor and Francis, London.